

Vibration Studies on BTeV Quadrupole Support Post

Giobatta Lanfranco, C.Boffo, F.McConolgue

*Fermi National Accelerator Laboratory
Technical Division – Engineering and Fabrication*

3rd March 2005

1. Abstract

The BTeV quadrupole post has the function to provide, besides thermal insulation, structural support for the cold mass. It is hence fundamental to determine the fundamental frequencies of the suspended cold mass system as well as the perturbing frequencies present in the environment where the quadrupole magnets will be installed. Vibration and ground motion measurements have been carried out in the C0 main assembly building pit and the results have been compared with a finite element model. A simple deflection test has been also performed and the elastic behavior of the support post verified.

2. Vibration test setup

The test stand must guarantee a rigid support to the system, in particular the vibration modes must be sufficiently far from what expected in the tested system. Several structures have been analytically studied, the requirement being a minimum natural frequency of 50Hz.

The first natural frequency for a beam simply supported and centrally loaded can be represented by the following relation

$$f_1 \propto \frac{1}{2\pi} \sqrt{\frac{EI}{L^3} \frac{1}{m_{\text{suspended_at_the_center}} + 0.486M_{\text{beam}}}}$$

Equation 1

where E is the modulus of elasticity, I the area moment of inertia, L the beam length, $m_{\text{suspended_at_the_center}}$ is a mass centrally suspended and M_{beam} the mass of the beam. From Equation 1 it is evident how the suspended mass dominates negatively the value of f_1 . The use of a simple “Stonehenge” concrete structure, although its mass still adversely affecting f_1 , has the advantage to achieve high levels of EI – and consequently f_1 – in a very economic way. This can be seen in Figure 1, where f_1 for the concrete structure is above 79Hz.

Figure 2 and Figure 3 show, respectively, a schematic and a real view of the chosen test stand.

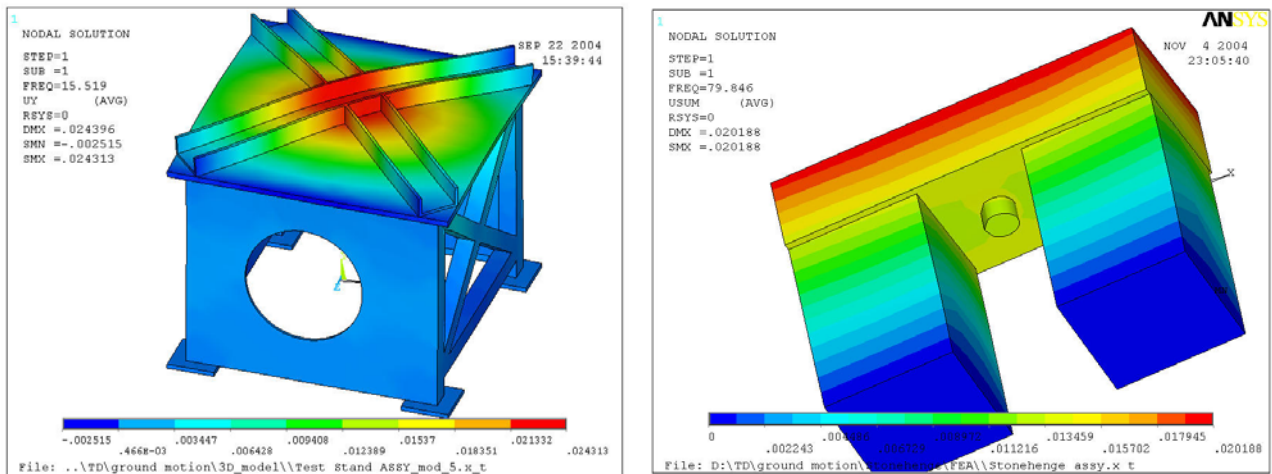


Figure 1 – Left: one of the various investigated solutions for a test stand in metal with an unacceptable 15.5 Hz first natural frequency. Right: the concrete stand used for the test, whose calculated first fundamental frequency is noticeably higher than the required 50 Hz. The suspended magnet mass is 3520 ± 20 lb (~1600 kg).

The top block was leveled and, in order to eliminate potential rocking, epoxy was used to fill the gaps between the top block and the two concrete feet. The epoxy was applied between plastic sheets to prevent the feet from adhering to the top and causing problems at the moment of disassembling the stand.

Stainless steel precision shim washers were used to level the concrete attachment plate (see assembly drawing 5525.000-ME-439041) before bolting it, via HIS Hilti threaded inserts, to the top block. The leveling accuracy was within 2 mils over the 14 inches of the plate. Figure 4 shows the mounting sequence of the support post fastening to the magnet.

The magnet mass attached to the post was 3520 ± 20 lb (~1600kg). Great attention has been paid to prevent the post from being stressed other than in tension. For this reason the magnet has been supported in correspondence of its center of gravity.

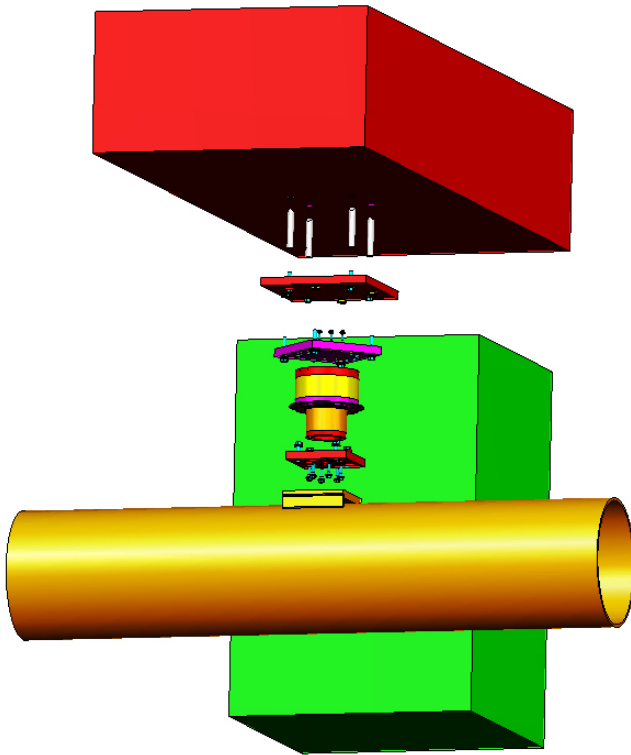


Figure 2 – Exploded view of the test setup.



Figure 3 – Complete view of the test setup. The three concrete shielding blocks make up the test stand structure. The magnet is hanging from the post. During the measurements, the two die carts, used to lift the magnet in place, were kept about 1/8 in below the suspended cold mass for safety.

The sensors used (see Figure 4) are:

- 3 GeoSpace HS-1 (2 horizontal 1 vertical):
4.5 Hz natural frequency 1.15 V/in/s sensitivity
- 1 Sercel Mark L4c:
1.0 Hz natural frequency 7.191 V/in/s sensitivity

The HS-1 sensors have been combined in a block in order to measure the vertical, transversal and longitudinal modes of vibration in different locations by keeping the same geometrical relative position of the sensors. The L4c is used as a reference for the ground vertical displacement. Data acquisition and analysis is performed using a MATLAB based custom application.

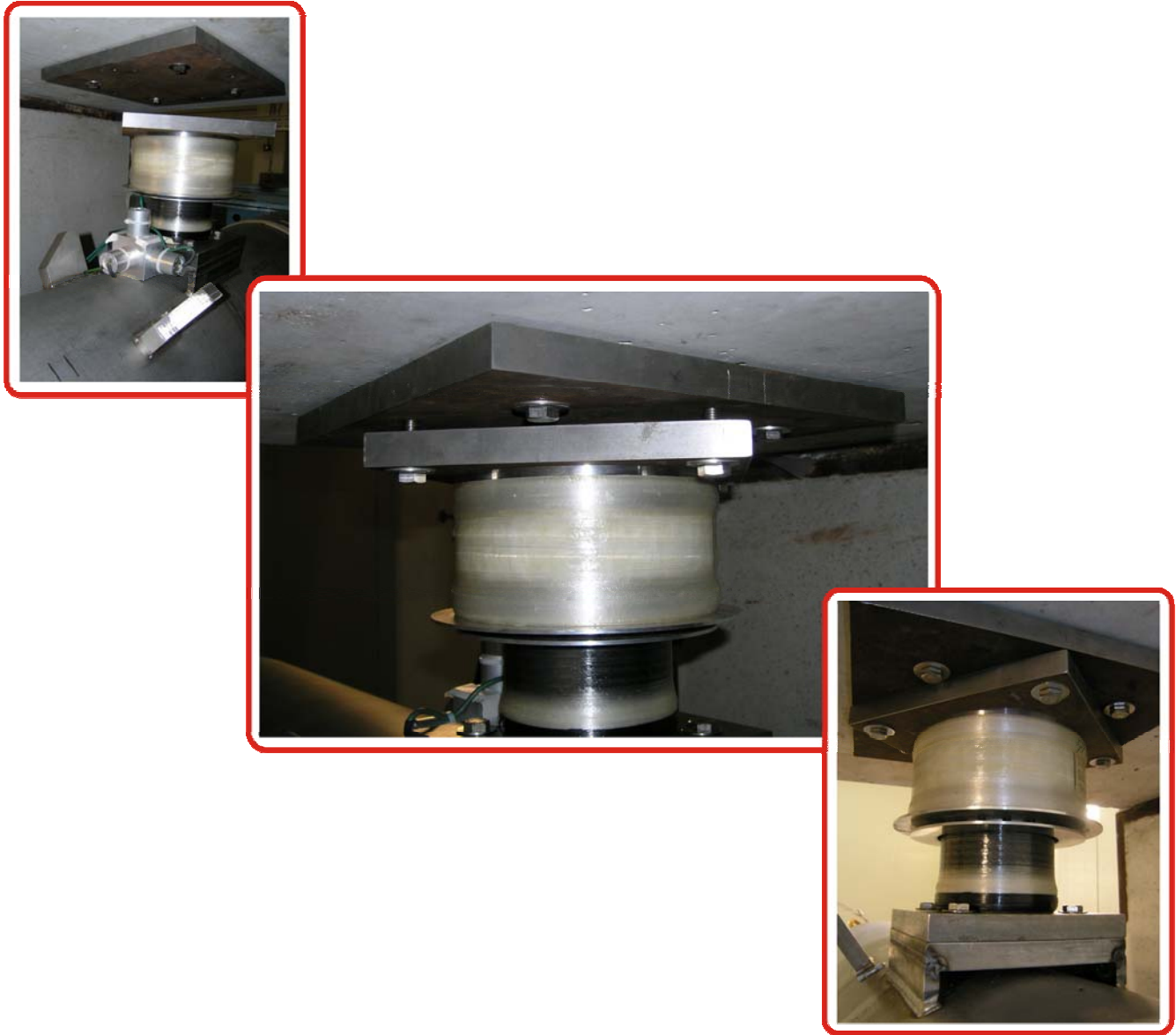


Figure 4 - The successive phases of the magnet anchoring to the top shielding block plate. The geophones used for the support post vibration study are clearly visible in the first frame.

3. Experimental Results

Ground motion data were acquired for about one hour per session during two separate sessions, Tuesday morning (22nd February 2005) and Friday late afternoon (25th February 2005), trying to see whether or not human activities, varying during the course of the week, might have had any impact on the perturbing frequencies at the C0 facility. No appreciable differences were noted among the two sessions.

Data were sampled at 100Hz. The three geophones used provided a reliable reading for frequencies above 3Hz.

In Figure 5 through Figure 7 the measured data are displayed. For each graph the traces color is black for the magnet longitudinal mode and blue for the magnet transversal mode; the red trace is the ground motion (floor vertical mode).

In particular, the ground motion in proximity of the test setup is charted in Figure 5. The perturbing frequencies were 9, 14, 18, 29.7, 59.5¹ Hz. At 18, 29.7 and 59.5 Hz the system was resonating.

Figure 6 and Figure 7 show the response of the magnet to a small bump (perturbing cause).

The system first four natural frequencies of vibration, in Hertz, were: 5.5, 18.0, 25.5, and 29.7. As expected, given the axial symmetry of the support post, no particular differences were observed between transversal and longitudinal excitation, amplitude aside².

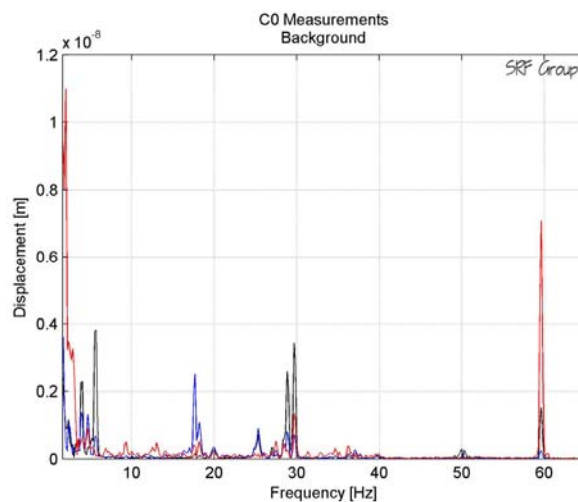


Figure 5 – Ground motion in proximity of the test stand.

Traces color. Black: accelerometer on magnet, longitudinal mode; blue: accelerometer on magnet, transversal mode; red: accelerometer on the floor, vertical mode.

¹ This frequency is clearly induced by asynchronous motors in the vicinity of the test operating at the line frequency.

² Due to the different impulse transmitted to the magnet.

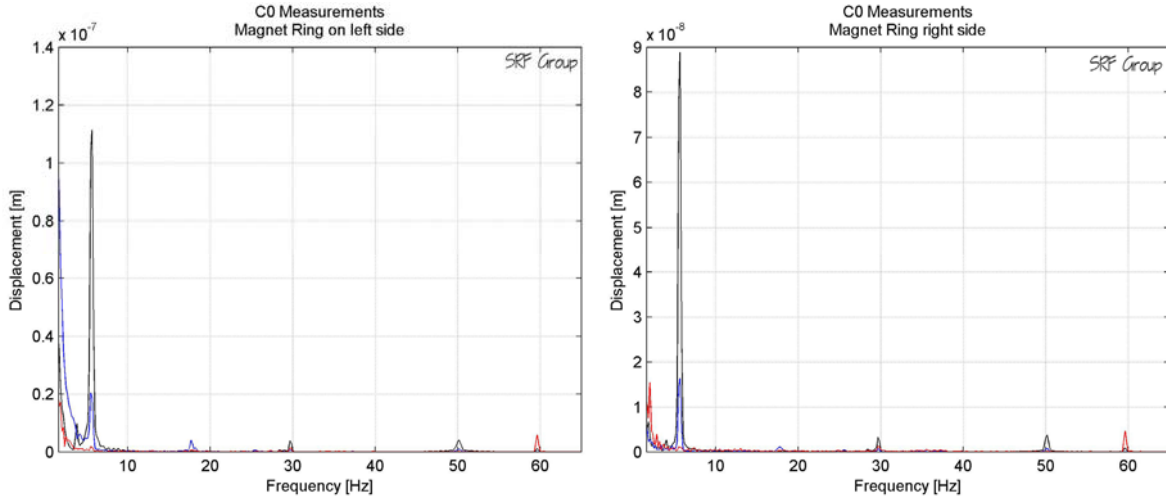


Figure 6 – Response of the magnet to a lateral perturbation (from both sides).
 Traces color. Black: accelerometer on magnet, longitudinal mode; blue: accelerometer on magnet, transversal mode; red: accelerometer on the floor, vertical mode.

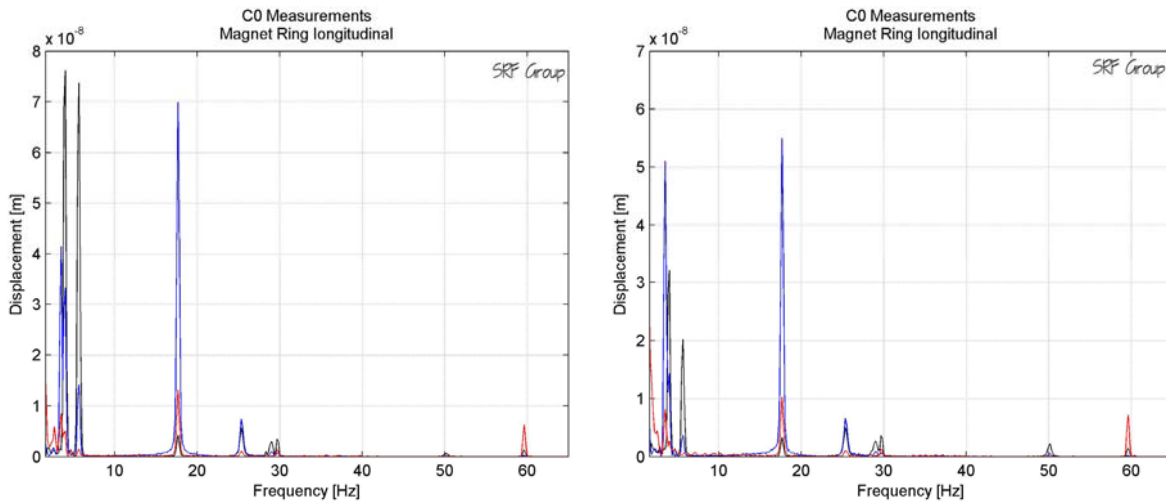


Figure 7 – Response of the magnet to a longitudinal perturbation (both directions). The system exhibits a similar³ behavior to what shown in Figure 6 for transversal excitation. The difference in amplitude respect Figure 6 is likely due to the different strength the magnet was hit.
 Traces color. Black: accelerometer on magnet, longitudinal mode; blue: accelerometer on magnet, transversal mode; red: accelerometer on the floor, vertical mode.

³ As expected given the axial symmetry of the support post.

4. Comparison with the finite element analysis

Uncertainties in the support post geometry have clearly undermined the value of the analytical verification, whose primary purpose was to determine the fiberglass damping coefficient. That would have allowed relying on the finite element method as an inferring tool for evaluating the system frequency response of fiberglass components.

Indeed, intention of the author was to section the post after the completion of the test, refine the 3D model used in the analytical formulation and rerun the analysis, fudging in the damping coefficient and converging towards what measured through an iterative process.

The suspended magnet has been modeled replacing the effective flange density with an equivalent one in order to keep into account the 3520lb. See Figure 8, top gray ring.

In

Table1 the properties of the support post fiberglass are shown. Figure 8 illustrates a 3D model of the simulated post while in Figure 9 it is possible to see the color contours of the first four vibration modes of the support post structure calculated via FEA.

Support Post Fiberglass properties

ρ	$2.768 \times 10^{-6} \text{ kg/mm}^3$ 0.1 lb/in ³
E	$2.76 \times 10^{10} \text{ Pa}$ $4 \times 10^6 \text{ psi}$
ν	0.3
G	$2.65 \times 10^9 \text{ Pa}$ 385000 psi

Table1. The support post fiberglass material properties.

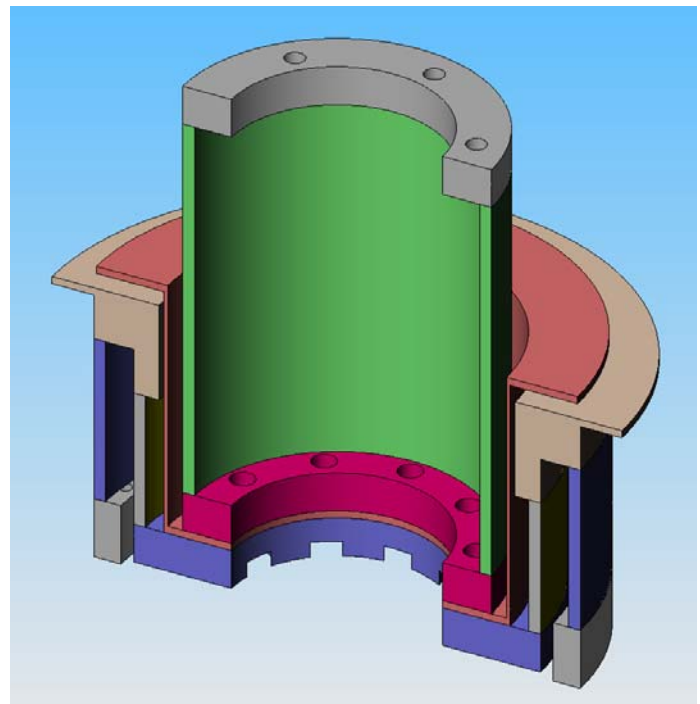


Figure 8 – 3D model of the simulated support post. Most of the internal dimensions were extrapolated clearly undermining the value of the analytical verification.

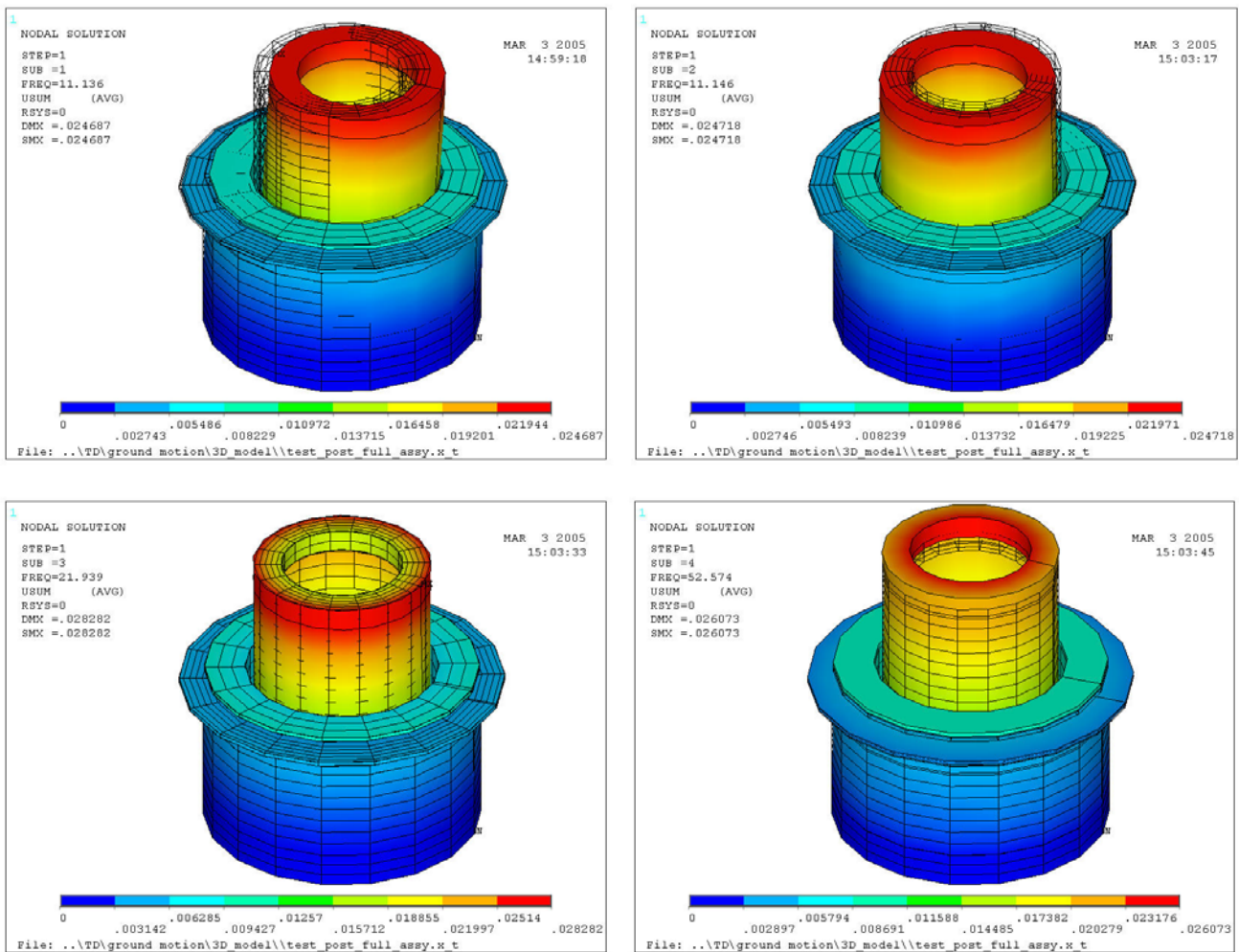


Figure 9 – From top left to bottom right, first four vibration modes of the support post structure calculated via FEA. The top flange equivalent density keeps into account the 3520lb of the suspended cold mass.

5. Load test

A very simple load test was also conducted. A hydraulic jack was mounted laterally, at the magnet center of gravity so as to apply a pure bending force on the support post. A dial indicator was placed diametrically opposed to the hydraulic jack with the intention to detect the consequent strain. In Figure 10 the applied force versus post strain is charted. The three load runs show a fairly good elastic response. The dial indicator was zeroed when the applied force was about 500N and that explains the offset of the origin.

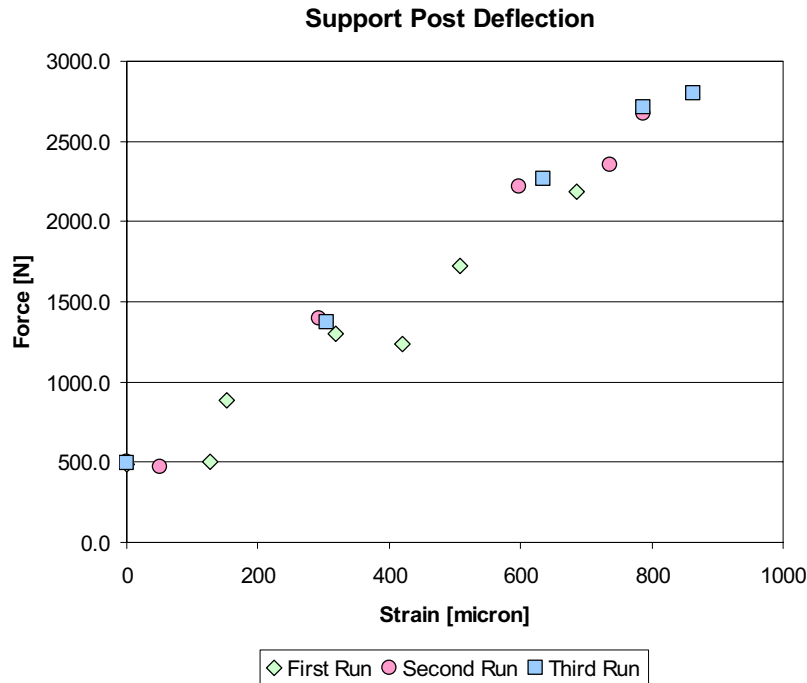


Figure 10 – Force versus strain in the support post simple load test. The dial indicator was zeroed when the applied force was about 500N causing the chart origin to offset.

6. Summary

The BTeV quadrupole support post was tested so as to determine the natural vibration modes of the suspended cold mass. The first four measured fundamental frequencies were 5.5 - 18.0 - 25.5 - 29.7 Hz. A quick ground motion study in the C0 main assembly building pit was also carried out, the perturbing frequencies found being 9, 14, 18, 29.7 Hz.

The analytical approach, intended to evaluate the fiberglass damping coefficient by the finite element method, is still a work in progress and underlines the necessity to adopt a 3D post model more correspondent to the real prototype.

Finally, a simple deflection test has been also performed and the elastic behavior of the support post verified. The cancellation of the BTeV project has prevented any further and conclusive investigation of the results.

7. Acknowledgments

A special appreciation for the very good work done goes to David Erikson, Otto Alvarez and Wojciech Blaszyński of the MAB machine shop, to Doug Kelley, Cliff Besch, Paul Mayer and Oscar Lira of the TD Material Control and finally to the C0 building manager Leonard Nelson.